Organic Electronics 13 (2012) 1470–1478

Contents lists available at SciVerse ScienceDirect

Organic Electronics

journal homepage: www.elsevier.com/locate/orgel

All-solution blade–slit coated polymer light-emitting diodes

Hongseok Youn [a], Kangmin Jeon [b], Seongbeom Shin [b], Minyang Yang [b,*]

[a] Department of Electrical Engineering and Computer Science, University of Michigan, 1301 Beal Avenue, Ann Abor, MI 48109, USA
[b] Department of Mechanical Engineering, Korea Advanced Institute of Science and Technology, 373-1 Guseong-dong, Yuseong-gu, Daejeon 305-701, Republic of Korea

ARTICLE INFO

Article history:
Received 1 February 2012
Received in revised form 15 March 2012
Accepted 5 April 2012
Available online 25 April 2012

Keywords:
Polymer light-emitting diodes
High-efficiency
Blade coating
Solution process

ABSTRACT

This paper reports that large-scale, all-solution processed, polymer, light-emitting diodes can be fabricated by a new blade–slit coating method under ambient conditions. It is practical to use an ionic solution and a ZnO nanoparticle solution as electron injection and electron transport materials, respectively, through a blade–slit coating system, and reduce the deviation of the layer thickness to less than one-third compared to the result of a conventional blade-only coating system. The standard deviations of the layer thickness coated by the blade–slit process were only 0.68 nm in the hole injection layer (PEDOT:PSS), and 2.3 nm in the polymer light-emitting layer (Super Yellow). In the case of blade-only coating, the standard deviations were 5.7 nm and 5.7 nm, respectively. The film non-uniformities of PEDOT:PSS and the Super Yellow layers fabricated by the blade–slit method were only 2.1% and 2.2%. In the case of blade-only coating, those were 7.9% and 9.1%, respectively. The application area was 80 mm × 70 mm. Moreover, because the devices do not contain any alkali or alkaline earth metals in the electron injection layer, they can be fabricated by an all-solution process in a normal air conditioned environment. The maximum luminous efficiency of all-solution blade–slit coated devices was as high as 5.26 cd/A without alkali metals, and the maximum luminance reached was 14 120 cd/m^2 at 7.8 V. These results are comparable to the performance of spin-coated devices.

1. Introduction

Recently, polymer light-emitting diodes (PLEDs) have attracted considerable interest due to their various advantages such as an easy solution process, low cost, and large-scale and high-throughput. Solution-processed PLEDs are now regarded as a promising technology for next-generation displays and solid-state lighting applications. However, the conventional electron injection layers are commonly fabricated by vacuum evaporation processes due to the vulnerability of these layers to oxygen and moisture in the air. Because the thickness of the electron injection layers such as LiF [1], CsF [2], NaF [3] is only around 1 nm, device performance levels are sensitive to the surface quality of the underlying layers when fabricated by a solution process. Owing to these critical problems, these ultra-thin electron injection layers are not appropriate for a solution process.

Many studies related to various fabrication technologies have been conducted to determine feasible processes for solution-processed OLEDs, such as simple printing and coating processes instead of vacuum processes. In particular, PLEDs and OPVs have been fabricated by spin coating, roll-to-roll printing [4,5], screen printing [6], and blade coating processes [7].

Because spin-coating requires simple components and has easy operational features, it is widely used in various areas of organic electronics, including PLEDs, organic photovoltaics (OPVs), and organic thin film transistors (OTFTs). However, with the spin-coating process, the larger the substrate, the greater the production cost, due to a low material utilization rate. Furthermore, the spin-coating process causes non-uniformity problems in larger devices.

* Corresponding author. Tel.: +82 42 350 3224.
E-mail address: myyang@kaist.ac.kr (M. Yang).

1566-1199/$ - see front matter © 2012 Elsevier B.V. All rights reserved.
http://dx.doi.org/10.1016/j.orgel.2012.04.008

The roll-to-roll process can also result in serious coating inhomogeneity and instability problems because the coating inks on the roll surface are in direct contact with the substrate. During the printing process, the direct contact between the ink and the substrate induces extensional viscose flows. Consequently, problems such as streak patterns [10] can occur, that in turn, cause both non-uniformity in the luminance and electrical shorting.

Due to printing instabilities of the direct contact printing process, the blade coating process has been considered a suitable non-contact process for multi-layer processed PLEDs [7]. In addition, blade coating has advantages in fabrication, such as being able to control film thickness by adjusting the solution concentration, the blade gap, or the blade speed.

Because of these advantages, the blade coating process is also widely used as a PLED coating process. However, most previous studies are limited to applying the blade coating process for fabricating only two layers such as a hole injection layer (HIL) and an active layer [5,6]. However, previously used soluble electron injection materials such as Cs_2CO_3 [9] and $Ca(acac)_2$ [12] have serious oxidation problems. In addition, various surfactant-like or water/alcohol-soluble ionic polymers [11,13–15] are easy to be aggregated on the hydrophobic surface of a light-emitting polymer layer, because most of these materials are dissolved into the polar solvents [16].

Furthermore, when higher molecular-weight polymers are used as light-emitting materials, the coating problems become more serious. In this paper, the ZnO nanoparticle (NP) is used as the electron transport layer, and to supply a practical hydrophilic surface for the next air-stable ionic solution containing ammonium cations as the electron injection layer.

The conventional blade coating processes incur serious problems related to the coating uniformity in the direction of coating because the ink supply rate is not constant.

In this paper, we suggest a blade–slit coating method, instead of a blade-only coating method, to fabricate large-scale PLEDs, and utilize a ZnO NP layer/ammonium ionic layer as an electron transport/injection layer. The hole injection layer, light-emitting polymer layer, and electron transport and injection layers were made by an all-solution process employing the blade–slit coating method. All processes were conducted under ambient air conditions. Furthermore, the efficiency of all-solution blade–slit coated PLEDs was comparable to that of the spin-coated PLEDs.

2. Experimental

The device structures of the PLEDs are indium tin oxide (ITO)/poly(3,4-ethylenedioxythiophene)poly-(styrenesulfonate) (PEDOT:PSS)/phenyl substituted poly(para-phenylene vinylene)—known as "Super Yellow", (S-Y, Merck, PDY-132)/zinc oxide (ZnO) nanoparticle (NP), poly(ethylene oxide) (PEO), and tetra-*n*-butylammonium tetrafluroborate ($TBABF_4$) in acetonitrile (ionic solution)/Al, as shown in Fig. 1.

The following is a summary of the fabrication process. Each layer was fabricated at a temperature of 45 °C on the hot plate under ambient air conditions. The blade–slit speed was 15 mm/s. Sputtered ITO glass (15Ω/□) was cleaned beforehand by an ultrasonic treatment in pure water, acetone, and isopropyl alcohol. It was then subjected to a UV–ozone treatment for approximately 1 h. A PEDOT:PSS layer (40 nm) was then blade–slit coated onto the ITO glass. The slit gap between the blade and the slide glass for the PEDOT:PSS layer was 70 μm. A yellow light-

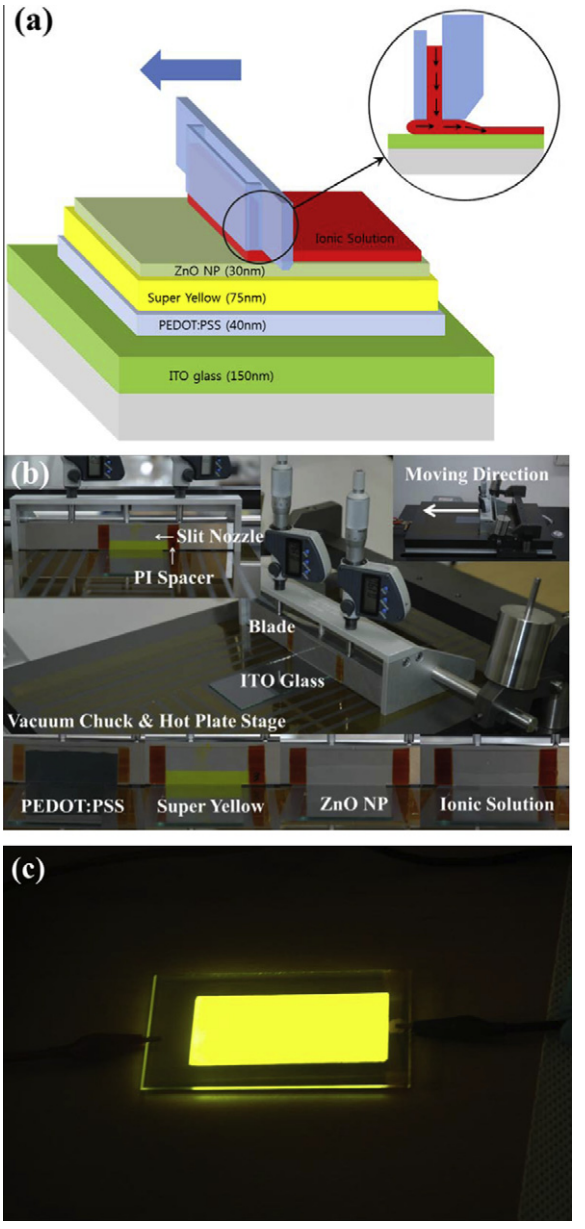

Fig. 1. (a) Illustration of the multilayer structure and the fluid flow along the blade, slide glass and substrate during the fabrication by the blade–slit coating method. (b) The image of the whole systems of the blade–slit coater, the image of the blade–slit nozzle (in left and top of the image) and the images of the blade slit nozzles containing various solutions for the PLEDs layers (in the bottom of the image). (c) The yellow light-emitting PLEDs on the ITO glass: substrate size, 100 mm × 50 mm. (For interpretation of the references to colour in this figure legend, the reader is referred to the web version of this article.)

emitting polymer (S-Y) dissolved in toluene at 0.6 wt.% was then blade–slit coated (approximately 75 nm). The slit gap between the blade and the slide glass for the S-Y layer was 210 μm. The ZnO NP layer (approximately 30 nm) was blade–slit coated onto the emissive layer. The ZnO NPs dispersed solution, dissolved in 1-butanol at a concentration of 30 mg/mL, was synthesized according to the method described by Beek et al. [17]. The slit gap between the blade and the slide glass for the ZnO NP layer was 210 μm. The ZnO NPs appeared rather monodispersed with an average size of approximately 5 nm. Finally, the ionic solution was blade–slit coated onto the ZnO NP layer. The slit gap between the blade and the slide glass for the ionic layer was 350 μm. The ionic solution containing $TBABF_4$ and PEO permeated into the ZnO NP layer, which was thin and porous after the ionic solution was blade–slit coated onto the ZnO NP layer. The aluminium cathode (100 nm) was thermally evaporated under 2×10^{-6} torr.

The device performance levels of the *J* (current density)–*V* (voltage)–*L* (luminance) curves were obtained from a Minolta CS-100 luminance meter and a Keithley 2400 source meter. The measurement process was conducted in ambient air conditions without encapsulation.

The thickness was measured by a surface profiler (Alpha step 500) through the height difference and with a resolution of 0.1 nm. And the thickness information of the cross-sectional scanning electron microscopy (SEM) images was acquired from Nova-230, a resolution of 1 nm at 20 kV.

3. Results and discussion

3.1. Description of the blade–slit coating method

Since the conventional blade coating system has advantages such as easy operation, simple structure and low cost, it has been widely used in not only laboratory scale but also industrials scale. Therefore, there have been lots of trials to make organic electronics using the simple blade coating due to these advantages. [5–8] The blade–slit coating system also employs the conventional blade coating system except the blade–slit nozzle. It consists of a coating nozzle, a hot plate, a vacuum chuck, and a moving stage as shown in Fig. 1(b). A serious problem of the conventional blade-only coating is that the ink is not supplied constantly. Accordingly, the layer thickness in the initial state is usually greater than that in the final state for a large-scale device. To avoid this problem, Chen et al. employed hot-blowing in the blade-only coating to make a uniform film. They reported that the uniformity of the film was around 10% in area of 50 mm × 50 mm [8].

In this paper, to achieve a better uniformity which is appropriate for much thinner organic layers such as the electron injection layer and to solve this fundamental ink supplying problem, a commercial slide glass (76 mm × 25 mm) was attached to the surface of a blade (200 mm × 28 mm) which was thermally annealed stainless steel as shown in Fig. 1(a). The solution contained in the slit began to flow and initially created the meniscus, then a laminar flow. This fine laminar flow is the key to uniformity and a better film quality. The control variables of the film thickness are the blade gap, the slit gap, the blade speed and the ink concentration. This coating mechanism is quite similar to the slot-die coating. However, the main difference between the blade–slit coating and the slot-die coating is the ink supply. The blade–slit coating system does not employ external pumping system. The conventional slot-die coater has a static pumping system to deliver the inks from the reservoirs containing sufficient amount of the inks to the slot nozzle. Because the pumping pressure is related to the flow rate, the pumping pressure of the slot-die coating is very important parameter to affect wet film thickness. And the static pressure of the pump has a decisive effect on the film uniformity. Furthermore, the organic electronic devices such as OPVs, OTFTs and OLEDs have very thin layers (from a few tens of nanometers to a few hundreds of nanometers) in their internal structure. Thus, it requires much smaller feeding capacity of the solution. To realize thin organic layers, some research groups, for example Kreb's group frequently employed a custom-made small slot-die nozzle and pumping system which can control a few microliters of solution and it is appropriate to make OPVs layers. [9] PLEDs in this paper, however, required much thinner film thickness for the ZnO NP layer/Ionic complex layer as an electron transport/electron injection layer (total thickness of the two layers is only from 15 nm to 30 nm). Therefore, it required much less and homogeneous amount of ink supply. In particular, it is hard to find the previous reports to fabricate the electron injection layer using the practical solution processes due to its ultra-thin (approximately 1 nm) layer thickness, vulnerability in the air and the aggregation problem on the hydrophobic active layer. In this paper, we aimed at fabricating four layers of not only the hole injection layer, emissive layer and electron transport layer but also the electron injection layer using by a new practical type of simple blade coating. The blade–slit coating can utilize the only natural gravity and surface tension of the solution to flow out from the capillary to the surface of the substrate when the other control parameters (blade speed and slit gap and blade gap, etc.) are fixed. Therefore, the blade–slit coating can effectively reduce the flow rate and the wet film thickness. The amount of the solution for each layer to be coated is only 25 μL in area of 50 mm × 50 mm. And whole volume of the slit space is 550 μL. In addition, it is inexpensive and easy to change and clean the nozzle for the different solutions. Since the blade–slit coating employs transparent slide glass for the slit capillary, it is quite useful to observe the fluids flows in the slit nozzle.

3.2. The results of the coating performances

For large-scale devices, the thickness of the blade-only coating is non-uniform in the coating direction, as shown in Fig. 2. Thickness variation is a serious problem associated with PLEDs, because a thickness difference in the functional layers, particularly a very thin electron injection layer causes a difference in the luminance, as shown in Fig. 2(e). Furthermore, an excessively thin area causes electrical-fatigue fracturing, manifested by electrical shorts in the PLED layers. Due to these problems with blade-only coating, the blade–slit coating method is suitable for

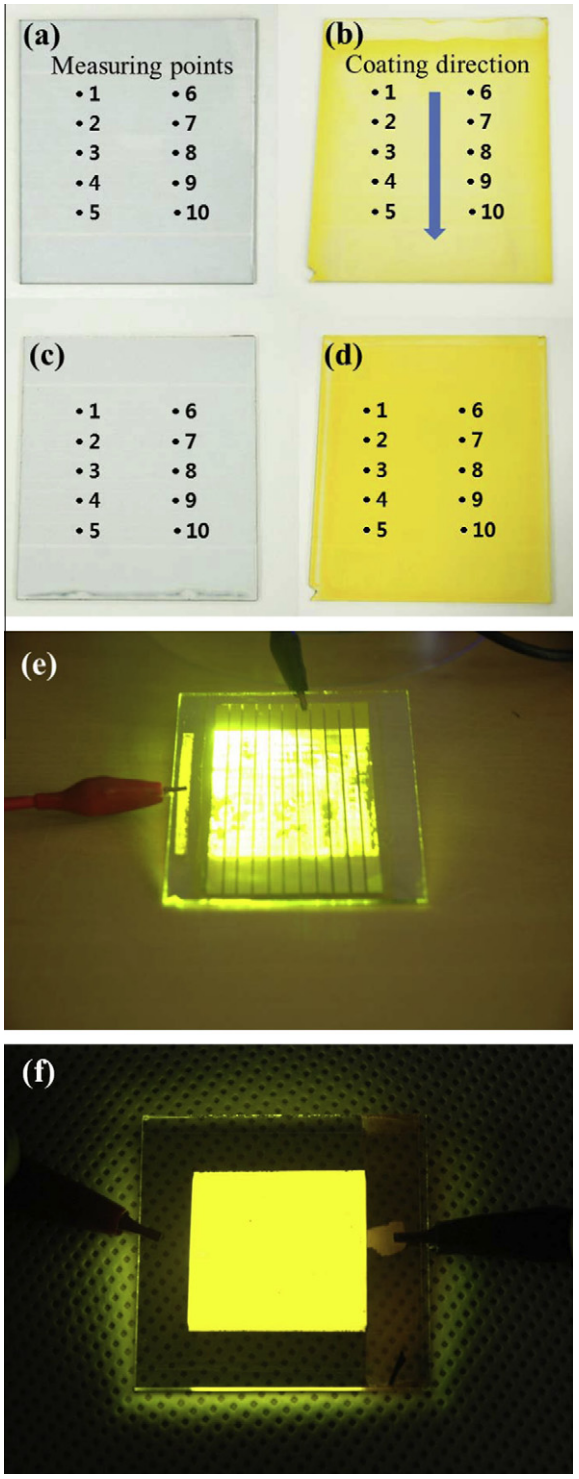

Fig. 2. (a) PEDOT:PSS layer coated by blade-only method and measuring points by surface profiler. (b) S-Y layer coated by blade-only method and showing coating direction. (c) PEDOT:PSS layer coated by blade–slit method. (d) S-Y layer coated by blade–slit method. (e) The image of non-uniform luminance fabricated by blade-only coating method. (f) The image of uniform luminance of the device fabricated by the blade–slit coating.

large-scale devices because it can supply the coating solution continuously and uniformly. Blade–slit coating improved the coating uniformity in the moving direction. The measured standard deviations of the blade-only coated PEDOT:PSS and S-Y layers were about 5.7 nm and 5.7 nm, respectively. Their non-uniformity measurements were around 7.9% and 9.1%, respectively. The non-uniformity was calculated from thickness data measured at 10 given positions (2 columns and 5 rows, each spaced 25 mm and 12 mm, respectively) in the area of the coated layer (substrate area: 70 mm × 80 mm), as shown in Fig. 2(a). The non-uniformity is represented by the standard deviation of the layer thickness divided by the average thickness in the film area. A smaller value of the non-uniformity implies better quality of film coating. See Table 1. The lack of the uniformity of the blade-only coated layers created serious non-uniform luminance when the device was driven as shown in Fig 2(e). However, Table 1 shows that the standard deviation of the blade–slit coated layer was only 0.68 nm and that its uniformity was 2.1% in PEDOT:PSS. It exhibited dramatic improvement in film uniformity when compared to the blade-only coating. In addition, the standard deviation of the S-Y is only 2.3 nm and its non-uniformity is 2.2%.

The devices fabricated by the blade–slit coating system successfully demonstrated large-cell-scale (substrate area: 100 mm × 50 mm) and all-solution-processed PLEDs as shown in Fig. 1(c). In addition, the film thickness of the various layers in the device could be controlled because the blade–slit coating method provides a continuous ink supply and a linear relationship between layer thickness and blade gap. See Table 2.

In Table 2, the film uniformity of the PEDOT:PSS and S-Y layers is dependent on film thickness. In particular, thicker film has greater uniformity than does the thinner film, as can be inferred from Table 2. Therefore, for a more fair and accurate evaluation of coating performance, the blade-only and blade–slit coating methods were compared when applied to layers of the same thickness. See Table 3. The non-uniformity measurements of blade–slit coating in the PEDOT:PSS and S-Y layers were 3.8% and 4.1%, respectively. Non-uniformities for blade-only coating were 7.9% and 9.1%, respectively. Given that layers of similar thicknesses were used in this case, we see that more than a two-fold improvement in film uniformity can be achieved.

To compare the coating performance with spin coating, the non-uniformity measurements for blade–slit coating in the PEDOT:PSS and S-Y layers were 2.1% and 4.3%, respectively. In the case of spin coating, the measurements were 4.4% and 4.8%. See Table 4. The film coating performance of the blade–slit method was quite similar in case of the S-Y layer and better in the PEDOT:PSS layer. Moreover, for large-scale devices, the blade–slit coating method is advantageous due to its better solution utilization rate.

Because the ZnO NP layers were too thin to evaluate, around 30 nm as measured by the surface profiler, these films needed to be investigated with scanning electron microscopy (SEM). Therefore, the thickness of the blade–slit coated ZnO layers as measured by the image of the SEM as shown in Fig. 3. The film thickness of the ZnO NP

Table 1
Film uniformity of PEDOT:PSS and Super Yellow layers for blade-only coating vs. blade–slit coating.

												Avg[a] (nm)	SD[b] (nm)	U[c] (%)
Blade only	Hole injection layer, PEDOT:PSS (nm)													
	Pos[d]	1	2	3	4	5	6	7	8	9	10			
	Thk[e]	73.1	79.3	71.6	76.7	75.0	78.0	73.3	61.1	63.2	73.1	72.4	5.7	7.9
	Light-emitting layer, Super Yellow (nm)													
	Pos[d]	1	2	3	4	5	6	7	8	9	10			
	Thk[e]	71.3	55.8	58.1	55.9	60.2	71.4	60.9	64.7	68.9	60.2	62.7	5.7	9.1
Blade slit	Hole injection layer, PEDOT:PSS (nm)													
	Pos[d]	1	2	3	4	5	6	7	8	9	10			
	Thk[e]	32.9	32.4	32.2	33.3	31.3	33.7	32.6	32.0	31.9	32.0	32.4	0.68	2.1
	Light-emitting layer, Super Yellow (nm)													
	Pos[d]	1	2	3	4	5	6	7	8	9	10			
	Thk[e]	102.2	100.0	102.9	105.4	104.3	102.2	100.2	100.1	106.1	105.7	102.9	2.3	2.2

[a] Avg: average thickness of ten points (nm).
[b] SD: standard deviation (nm).
[c] U: non-uniformity (%): (SD/Avg).
[d] Pos: measured position.
[e] Thk: thickness.

Table 2
Film uniformity of PEDOT:PSS and Super Yellow layers coated by blade–slit method.

Layers	Blade gap (μm)	Avg[a]	SD[b]	U[c]
PEDOT:PSS	20	48.3	2.5	5.2
	30	75.7	2.5	3.8
	40	107.7	1.5	1.4
S-Y	30	60.7	2.5	4.1
	40	98.3	1.5	1.5
	50	146.7	2.1	1.4

[a] Avg: average thickness of ten points (nm).
[b] SD: standard deviation (nm).
[c] U: non-uniformity (%): (SD/Avg).

Table 3
Film uniformity of PEDOT:PSS and Super Yellow layers coated by blade-only and blade–slit coating methods.

Coating method	Layers	Blade gap (μm)	Avg[a]	SD[b]	U[c]
Blade coating	PEDOT:PSS	30	72.4	5.7	7.9
	S-Y	30	62.7	5.7	9.1
Blade–slit coating	PEDOT:PSS	30	75.7	2.5	3.8
	S-Y	30	60.7	2.5	4.1

[a] Avg: average thickness of ten points (nm).
[b] SD: standard deviation (nm).
[c] U: non-uniformity (SD/Avg%).

Table 4
Film uniformity of PEDOT:PSS and Super Yellow layers coated by spin-coating method.

Coating method	Layers	Spin rate (rpm) Blade gap (μm)	Avg[a]	SD[b]	U[c]
Spin-casting	PEDOT:PSS	2000	39.5	2.1	4.4
	S-Y	2500	54.0	2.6	4.8
Blade–slit coating	PEDOT:PSS	10	32.4	0.68	2.1
	S-Y	25	57.7	2.5	4.3

[a] Avg: average thickness of ten points (nm).
[b] SD: standard deviation (nm).
[c] U: Non-uniformity (SD/Avg%).

layer was controlled by adjusting the blade gap distance. See Table 5. The thicknesses of the blade–slit coated Super Yellow layer and ZnO NP layer were linearly proportional to the blade gap distance when the other control variables

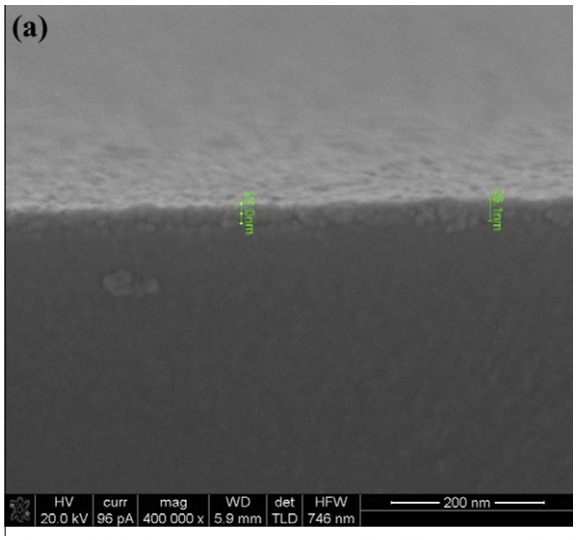

Fig. 3. (a) The SEM image of ZnO NP layer (29.1 nm) coated by the blade–slit method with a concentration of 30 mg/mL ZnO NP solution on the glass substrate. (b) The SEM image of the ZnO NP layer (56.8 nm) coated by the blade–slit method with a concentration of 60 mg/mL ZnO NP solution on the glass substrate.

were fixed. The thickness of the ZnO NP layer, using a 30 mg/mL ZnO solution, also increased from 45 nm to 65 nm when the blade gap was increased from 45 μm to 65 μm. See Table 5. Surprisingly, the very thin ZnO NP layers can also be controllable.

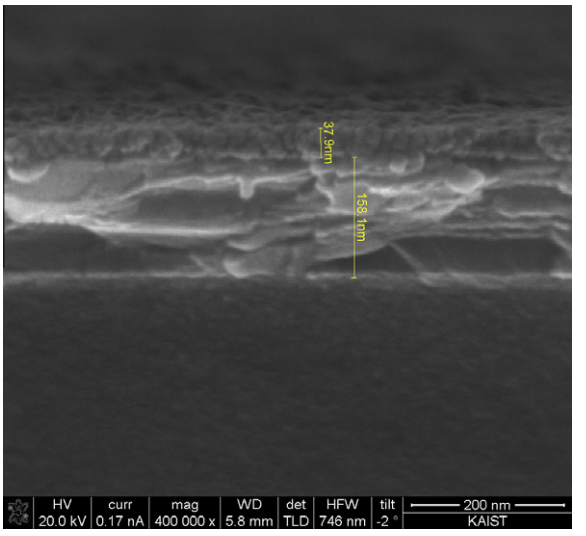

Fig. 4. The SEM image of the ZnO NP/ionic complex layer (37.9 nm) after the ionic solution ($TBABF_4$ + PEO) was blade–slit coated onto the ZnO NP layer coated on the ITO (158.1 nm) glass.

In case of S-Y layer, the thickness results of the S-Y layer from SEM analysis matched well with results from those of the surface profiler in Table 2. The thickness of the light-emitting polymer layer increased from 60.0 nm to 91.0 nm as the blade gap was increased from 30 μm to 40 μm in Table 5.

Adjustment of the solid concentration of the ZnO NPs is more effective in controlling film thickness than is adjustment of the blade gap. With the same blade gap, the film thickness with a solution concentration of 60 mg/mL is almost twice that of a solution concentration of 30 mg/mL. The thicknesses are 57.8 nm and 29.1 nm, respectively, as shown in Fig. 3. Moreover, the ionic solution containing the ammonium ions and PEO were well blade–slit coated and infiltrated into the ZnO NP layer, and then formed a ZnO NP/ionic complex as shown in Fig. 4. This implies the ZnO NP layer supplies a good hydrophilic surface. In addition, because this ionic solution (TBABF4 + PEO) does not contain any alkali or alkaline-earth metal, it is relatively stable in the air. Moreover, the ammonium cations (tetra-butyl ammonium) in the ionic solution create the interface dipole with the aluminium cathode. The interface dipole effectively shifts the aluminium work-function and then reduces the electron injection barrier [18]. PEO has a role of solid-state electrolyte which helps the ions move within the ZnO NP/ionic complex layer.

Table 5
Thickness variations of layers for blade–slit coating method with respect to gap distance between blade and substrate.

Super Yellow		ZnO nanoparticle	
Blade gap (μm)	Film thickness (nm)	Blade gap (μm)	Film thickness (nm)
30	60.0	45	15.3
35	75.0	55	20.4
40	91.0	65	30.0

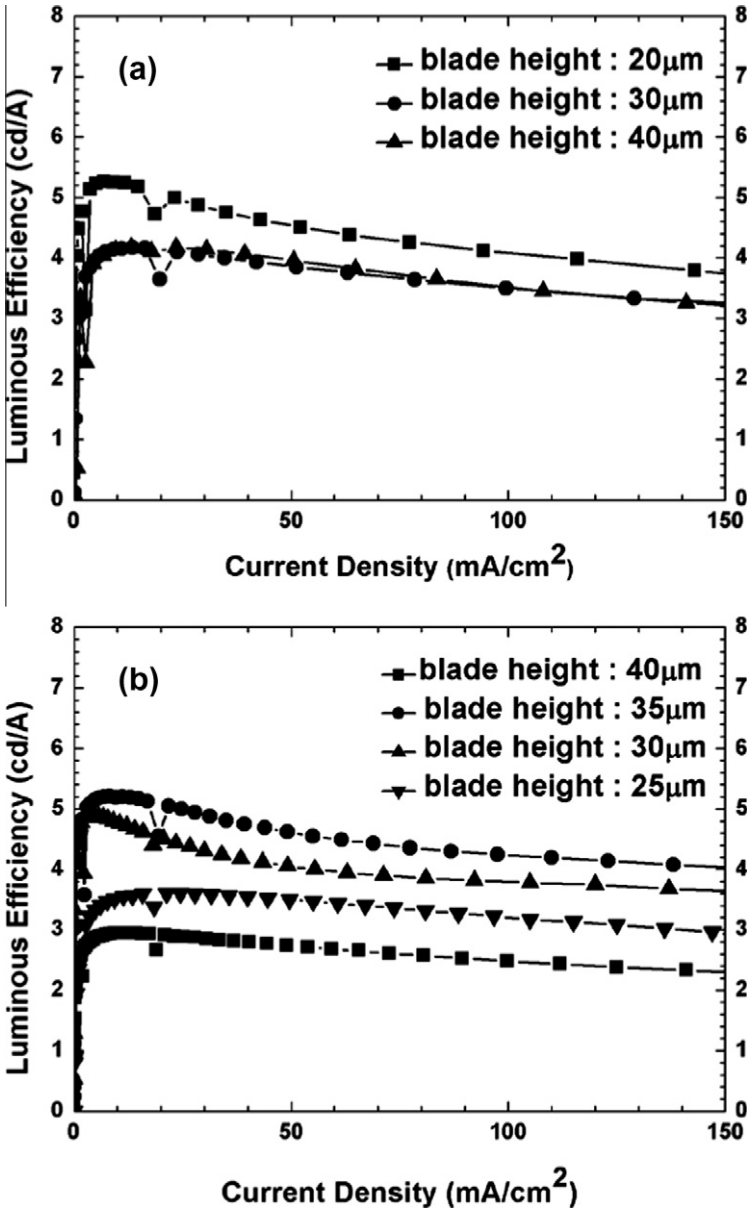

Fig. 5. Luminous efficiency as a function of thicknesses of (a) PEDOT:PSS layer and (b) emissive layer (S-Y).

The optimum film thickness for blade–slit coating of the ZnO NP and ionic complex layer was determined to be around 30 nm when using a 30 mg/mL ZnO NP solution and 0.15 wt.% ionic solution.

3.3. The results of the device performances

Fig. 5(a) shows performance levels of PLEDs using different blade gap distances in the PEDOT:PSS layer. The maximum luminance was 14120 cd/m^2 at 7.8 V with a device area of 6 mm^2, and the maximum luminous efficiency was 5.26 cd/A at a blade gap distance of 20 μm. However, the luminous efficiency decreased when the blade gap was more than 20 μm. Fig. 5(b) shows the different performance levels of OLED devices created with different blade gap distances in the S-Y layer. The maximum luminous efficiency was 5.26 cd/A at a blade gap distance of 35 μm. The luminous efficiency decreased when the thickness of the S-Y layer was thinner or thicker than 100 nm. We decided the optimal thickness of the other functional layers and checked the controllability of the coated layer thicknesses of the ZnO NPs layer and the ionic layer.

The conventional PLEDs have been fabricated by the spin-coating process because it is easier to do on a small scale in a laboratory. Furthermore, most highly efficient PLEDs are fabricated by the spin-coating process [18]. For a more accurate and fair comparison of blade–slit coating

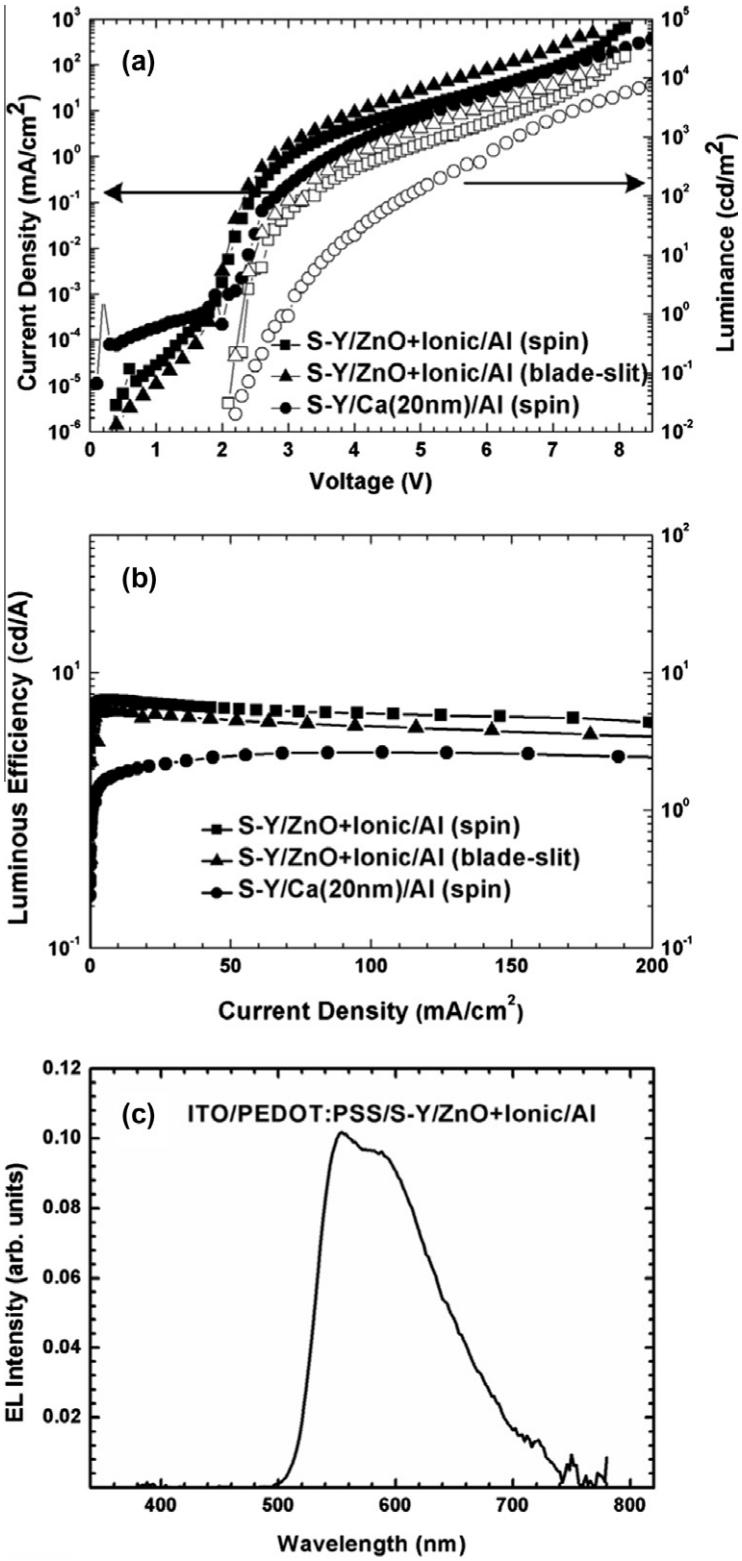

Fig. 6. (a) Current density, voltage, and luminance (*J*–*V*–*L*) characteristics with the spin-coated, the blade–slit coated and the spin-coated Ca (20 nm)/Al devices. (b) Luminous efficiency of the spin-coated, the blade–slit coated and the spin-coated Ca(20 nm)/Al devices. (c) The electroluminescence spectra at a voltage of 5 V.

and spin coating, the layer thicknesses of the two devices were kept similar. As a result, the turn-on-voltages and the maximum luminance voltage of the two devices were almost the same, as shown in Fig. 6(a). This suggests the blade–slit coating method can realize the same coating quality of spin coating in a larger size. In addition, Fig. 6(b) shows the performances between spin-coated devices and blade–slit coated devices. Though the blade–slit coated device was made in the air, the luminous efficiency of the blade–slit coated and spin-coated sample reached 5.26 cd/A. The luminous efficiency of the spin-coated device fabricated in the glove-box was 6.30 cd/A. These results support the advantage of the blade–slit coating method because results are comparable to the spin-coating method in terms of luminous efficiency, and blade–slit coating is easier and less wasteful of materials for large-sized devices (100 mm $\times$ 50 mm). Whereas, the luminous efficiency of the ITO/PEDOT:PSS/SY/ZnO + $TBABF_4$ + PEO/Al device is higher than that of the ITO/PEDOT:PSS SY/Ca(20 nm)/Al device with the value of 6.30 vs. 3.01 cd/A as shown in Fig. 6(b). And the turn-on voltages of the two devices are almost same as 2.2 V as shown in Fig. 6(a). Since the maximum wavelength of the S-Y in the EL-spectra is 560 nm as shown in Fig. 6(c), the optical band gap of the S-Y is calculated at 2.2 eV, the same as turn-on voltage. It means that the devices have a good electrical contact with Al cathode. In addition, it reveals that the ammonium ions effectively can be formed into a good interfacial layer as the electron injection layer which lowers the electron injection barrier instead of the alkali or alkaline earth metals.

4. Conclusion

We have successfully demonstrated that the fabrication of all-solution blade–slit coated polymer light-emitting diodes (PLEDs) is practical for large-sized devices (100 mm $\times$ 50 mm) in ambient conditions. The performance of blade–slit coated PLEDs was also comparable to the performance of spin-coated PLEDs. The maximum luminous efficiency of all-solution blade–slit coated devices was 5.26 cd/A even without any alkali or alkaline earth metals. The maximum luminance reached 14 120 cd/m^2 at 7.8 V. The standard deviations of the layer thickness coated by the blade–slit method was recorded as about 0.68 nm in the hole injection layer (PEDOT:PSS) and 2.3 nm in the polymer light-emitting layer (Super Yellow). The non-uniformities of PEDOT:PSS and Super Yellow layer was only 2.1% and 2.2% over an area of 80 mm $\times$ 70 mm. In the case of blade-only coating, those were 7.9% and 9.1%, respectively. The blade–slit coating method exhibited remarkable improvements over both the blade-only coating and spin coating methods. Moreover, we expect the blade–slit coating method can be used as a practical approach in fabricating large-scale devices.

Acknowledgements

This research was supported by KAIST EEWS (EEWS: Energy, Environment, Water and Sustainability) Flagship Research Project (2011) and the Fostering Next-generation Researchers Program through the National Research Foundation of Korea (NRF) funded by the Ministry of Education, Science and Technology (D00016).

References

[1] C. Wu, G. Lee, T. Pi, Appl. Phys. Lett. 87 (2005) 212108.
[2] G. Li, J. Shinar, Appl. Phys. Lett. 83 (2003) 5359–5361.
[3] J. Lee, Y. Parka, D.Y. Kim, H.Y. Chu, H. Lee, L.M. Do, Appl. Phys. Lett. 82 (2003) 173–175.
[4] Frederik C. Krebs, Org. Electron. 10 (2009) 761–768.
[5] P. Kopola, M. Tuomikoski, R. Suhonen, A. Maaninen, Thin Solid Films 517 (2009) 5757–5762.
[6] D.-H. Lee, J.S. Choi, H. Chae, C.-H. Chung, S.M. Cho, Displays 29 (2008) 436–439.
[7] Shin-Rong Tseng, Hsin-Fei Meng, Kuan-Chen Lee, Sheng-Fu Horng, Appl. Phys. Lett. 93 (2008) 153308.
[8] Chun-Yu Chen, Hao-Wen Chang, Yu-Fan Chang, Bo-Jie Chang, Yuan-Sheng Lin, et al., J. Appl. Phys. 110 (2011) 094501.
[9] Jan Alstrup, Mikkel Jørgensen, Andrew J. Medford, Frederik C. Krebs, ACS Appl. Mater. Interfaces 2 (2010) 2819–2827.
[10] J. Jasper, Suzanne H.P.M. de Winter, Laurence H.G. Symonds, Org. Electron. 10 (2009) 1495–1504.
[11] Jinsong Huang, Gang Li, Elbert Wu, Qianfei Xu, Yang Yang, Adv. Mater. 18 (2006) 114–117.
[12] Xu Qianfei, Jianyong Ouyang, Yang Yang, Appl. Phys. Lett. 83 (2003) 4695–4697.
[13] H. Wu, F. Huang, Y. Mo, W. Yang, D. Wang, J. Peng, Y. Cao, Adv. Mater. 16 (2004) 1826–1830.
[14] Y. Zhang, F. Huang, Y. Chi, A.K.Y. Jen, Adv. Mater. 20 (2008) 1565–1570.
[15] S.H. Oh, D. Vak, S.I. Na, T.W. Lee, D.Y. Kim, Adv. Mater. 20 (2008) 1624–1629.
[16] Yong Zhang, Fei Huang, Yun Chi, Alex K.-Y. Jen, Adv. Mater. 20 (2008) 1565–1570.
[17] W.J.E. Beek, M.M. Wienk, M. Kemerink, X. Yang, R.A.J. Janssen, J. Phys. Chem. B 109 (2005) 9505–9516.
[18] Hongseok Youn, Minyang Yang, Appl. Phys. Lett. 97 (2010) 243302.